

# A Stochastic Model for Optimizing Physical Carrier Sensing and Spatial Reuse in Wireless Ad Hoc Networks

Hui Ma, Hamed M. K. Alazemi\*, Sumit Roy  
Department of Electrical Engineering  
University of Washington  
Seattle, WA 98195, USA  
{mahui, hamed, roy}@ee.washington.edu

**Abstract**—The choice of Physical Carrier Sensing (PCS) threshold is key to the trade-off between the amount of spatial reuse and probability of packet collisions in a wireless ad hoc network. In this paper, we present a new analytical approach for optimizing the PCS threshold as measured by probability of packet collisions and the aggregate one-hop throughput. Our model simultaneously incorporates the impact of PCS threshold and the backoff mechanism via a suitable Markov chain model for saturation (i.e. all nodes always have a packet to send in their queues). Elaborate OPNET simulation results show the effectiveness of the analytical model.

**Keywords**—spatial reuse; physical carrier sensing; MAC; ad hoc network; IEEE 802.11; analytical modeling; simulation

## I. INTRODUCTION

Wireless ad hoc mesh (or multihop) networks that provide broadband connectivity to the backbone Internet for mobile clients in various environments such as campus, office and home must exploit the limited system bandwidth available via spatial reuse to enhance aggregate 1-hop throughput<sup>1</sup>. However, enhancing spatial reuse in such **dense** ad hoc networks depends on various factors [1]: the type of radio, signal propagation environment and network topology. In particular, the random topology of an ad hoc network has a significant impact on interference management and can cause large local variability in achievable spatial reuse.

In IEEE 802.11 WLANs, Distributed Coordination Function (DCF) [16-18] or CSMA/CA uses carrier sensing to determine if the shared medium is available before transmitting. Two types of carrier sensing are supported by DCF: mandatory physical carrier sensing (PCS) that monitors the RF energy level in the channel and optional virtual carrier sensing (VCS) that uses the request to send/clear to send (RTS/CTS) handshake to reserve the channel prior to data transmission. VCS is *presumed* to avoid the well known

hidden terminal problem [2] but solves this imperfectly at best, sometimes at the cost of enhancing the exposed terminal problem (needlessly suppressing allowable simultaneous transmissions) [4, 5, 14]. Accordingly, in [7] we have argued that a suitably chosen PCS mechanism may supplant the need for VCS in most practical scenarios.

Nodes using PCS sample the energy level in the medium and initiate channel access only if the signal power detected is below the PCS threshold. Although many of today's 802.11 hardware use static PCS threshold, prior research [6-8, 14] has recommended tuning PCS threshold to achieve a trade-off between the amount of spatial reuse and the probability of packet collisions, thereby improving the overall network throughput.

Our goal for this work lies in developing an analytical model for PCS tuning to evaluate its impact on network metrics such as the saturation throughput and the probability of collisions. There exists no credible analytical model *where the impact of network topology on PCS threshold selection has been considered*. We develop a Markov chain model that uses the PCS threshold and the contention window size as parameters to achieve the above.

## II. LINK LAYER MODEL

The common path loss model relates the average power at a receiver as a function of the transmitter-receiver separation distance,  $d$  via

$$P_{rx} = \bar{P}_{rx} \left(\frac{d}{\bar{d}}\right)^\gamma \quad (1)$$

where  $\gamma$  is path loss exponent and  $\bar{P}_{rx}$  is the power received at a reference point in the far field region at distance  $\bar{d}$  from the transmitting antenna.

Following [6], the aggregate energy at any receiving node consists of the desired signal, the interference (from unwanted transmitter(s)) and the background noise. A node can receive a packet with high probability of success only if a) the received signal strength is greater than a threshold (denoted by  $P_R$ , i.e.

<sup>1</sup> The aggregate throughput is proportional to the number of simultaneous communications in spatially separated locations.

\* H. Alazemi is Assistant Professor, Dept. of Computer Engineering at Kuwait University. This work was performed while he was a visiting faculty with Dep. of Electrical Engineering, U. Washington

This work was supported in part by a gift from Intel Research Council.

**reception sensitivity**) and b) the received Signal-to-Noise Ratio (SNR) exceeds a threshold denoted by  $S_0$ . Accordingly, the **transmission range**  $R$  defined as the maximum transmitter-receiver separation distance within which a packet is successfully received in the presence of no interference, is given by

$$R = \bar{d} \left( \frac{\bar{P}_{rx}}{\max(P_N S_0, P_R)} \right)^{\frac{1}{\gamma}} \quad (2)$$

where  $P_N$  is Background Noise Power. Note that in order to increase the number of simultaneous transmissions for better spatial reuse, one can set  $P_R$  to be higher than  $P_N S_0$  to keep  $R$  small. In this case, the transmissions become less vulnerable to interference and the transmission range

$$R = \bar{d} \left( \frac{\bar{P}_{rx}}{P_R} \right)^{\frac{1}{\gamma}} \quad (3)$$

The **carrier sensing range**  $X$ , defined as the distance within which a node will detect an existing transmission with high probability via PCS, is given by

$$X = \bar{d} \left( \frac{\bar{P}_{rx}}{P_C} \right)^{\frac{1}{\gamma}} \quad (4)$$

where  $P_C$  is the carrier sense threshold. Hence,  $R$  and  $X$  are related via

$$X = \left( \frac{P_R}{P_C} \right)^{\frac{1}{\gamma}} R \quad (5)$$

Furthermore, the **interference range**  $I$ , defined as the maximum distance at which the receiver will be interfered with by another source (i.e. the received SNR at reference receiver drops below the threshold  $S_0$ ) is given by

$$I = \left( \frac{1}{\frac{1}{S_0} - \left(\frac{d}{\bar{d}}\right)^{\gamma} \frac{P_N}{P_{rx}}} \right)^{\frac{1}{\gamma}} d \approx S_0^{\frac{1}{\gamma}} d \quad (6)$$

where the second expression assumes negligible background noise.

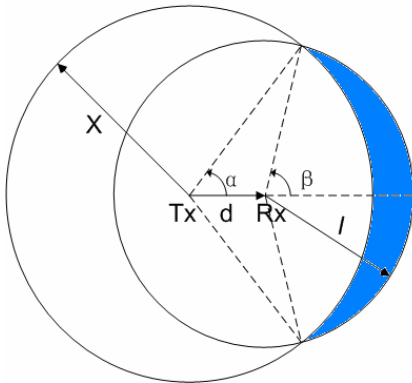


Figure 1. Geometry of carrier sensing area and interference area

From Figure 1, since the carrier sensing area of the transmitter (circle centered at TX with radius of  $X$ ) does not coincide with the interference area of the receiver (circle centered at RX with radius  $I$ ), any node within the interference range of the receiver but outside the carrier sense range of the transmitter is potentially a hidden terminal [2]. Likewise, any node within the carrier sense range of the transmitter but outside the interference range of the receiver becomes an exposed terminal [3].

The “hidden” area to the sender, denoted by  $A(d)$  can be expressed in terms of  $d$ ,  $X$  and  $I$  as

$$A(d) = \begin{cases} 0 & (X \geq I + d) \\ \beta I^2 + dX |\sin(\alpha)| - \alpha X^2 & (I - d \leq X \leq I + d) \\ \pi(I^2 - X^2) & (X \leq I - d) \end{cases} \quad (7)$$

where  $\alpha = \cos^{-1} \left( \frac{X^2 + d^2 - I^2}{2dX} \right)$ ,  $\beta = \pi - \cos^{-1} \left( \frac{d^2 + I^2 - X^2}{2dI} \right)$

Equation (7) can be rewritten as

$$A(d) = \begin{cases} 0 & (0 \leq d \leq d_0) \\ \beta I^2 + dX |\sin(\alpha)| - \alpha X^2 & (d_0 \leq d \leq \min\{R, d_1\}) \\ \pi(I^2 - X^2) & (d_1 \leq d \leq R) \end{cases}$$

with  $d_0 = \frac{1}{1 + S_0^{\frac{1}{\gamma}}} \left( \frac{P_R}{P_C} \right)^{\frac{1}{\gamma}} R$  and  $d_1 = \frac{1}{S_0^{\frac{1}{\gamma}} - 1} \left( \frac{P_R}{P_C} \right)^{\frac{1}{\gamma}} R$

(8)

From the above, we can see that when  $d \leq d_0$ ,  $A(d) = 0$ , i.e., the interference area of the receiver is contained in carrier sensing area. However, when  $d$  increases, both the “hidden” area  $A(d)$  and interference range  $I$  increase as well, thereby, the hidden terminals in  $A(d)$  may lead to increased packet collisions.

We may be tempted to reduce  $A(d)$  and the hidden terminal problem by increasing carrier sense range  $X$ ; however the exposed terminal problem becomes more pronounced in this case, which prevents simultaneous transmissions and reduces spatial reuse. Therefore, tuning PCS threshold  $P_C$  (i.e. equivalent to tuning  $X$ ) directly affects both the hidden and the exposed node problem, which have opposing effects on the system throughput. Clearly, this inherent tradeoff lies at the core of optimizing the performance of multihop ad hoc networks by balancing the number of simultaneous transmissions in the system and the probability of packet collision at any node.

### III. SYSTEM MODEL FOR PCS

Motivations for our model may be traced to the Markov model developed for optimal transmission range in a multihop wireless network and used subsequently in to derive the saturation throughput of non-persistent CSMA and some variants of busy tone multiple access (BTMA) [11,12]. However, these models do not consider the effect of PCS threshold – therefore, a new Markov model which captures the effect of PCS threshold choice on the one-hop aggregate

network throughput is needed. Implicitly, this requires modeling channel status in both space and time.

We assume that collisions occur mainly due to hidden terminals of the senders; secondarily they may occur due to 'intrinsic' properties of the 802.11 MAC – i.e., several nearby nodes select the same slot to transmit. Since ACK packets are much smaller than data packets and typically transmitted using the lowest (most reliable) data rate, the probability of successfully receiving a data packet but losing an ACK is assumed to be negligible. Furthermore, we assume that nodes are distributed over the 2-D plane obeying the two-dimensional homogenous Poisson distribution with density of  $\lambda$ , i.e., for any given area  $S$ , the probability of the number of nodes  $N$  is given by

$$P(N = n) = \frac{(\lambda S)^n}{n!} e^{-\lambda S} \quad (9)$$

From the above assumptions, the channel status around any node A in the network can be modeled as a four-state Markov chain. This model reflects the characteristic of 802.11DCF (which is modeled as p-persistent CSMA [10]) inclusive of the PCS threshold, which is different from the model in [11, 12] for non-persistent CSMA. In particular, we consider the channel status within the carrier sensing range of node A, instead of the transmission range; we combined the two Markov chain models in [12] (one for channel status, the other for node activity) into one Markov chain model by introducing a new state — the Deferring state. As shown in Figure 2, the channel status of any node may be described as follows:

- The Idle state: the channel around reference node A is sensed idle, and its duration  $T_i$  is the length of an empty time slot defined in the IEEE 802.11 standard.
- The Success state: the channel is occupied with a successful transmission from node A for duration  $T_s$ .
- The Fail state: the channel is occupied with an unsuccessful transmission from node A (either due to hidden terminals or intrinsic reasons) for duration  $T_f$ .
- The Deferring state: the channel around node A is occupied with transmission from other nodes; thus node A freezes its backoff counter and defers its access until the channel around node A is sensed idle again. In this state, node A can also be a receiver. We denote the duration of deferring as  $T_d$ .

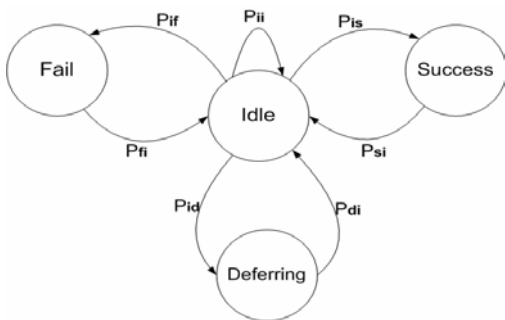


Figure 2. Markov chain model for channel status around any node A

Our work follows the Markov model of DCF in [9] where  $T_i, T_s, T_f$  and  $T_d$  to denote a generic time slot duration of the channel around node A in the various states<sup>2</sup>. Note that a busy channel will revert to the idle state after duration of  $T_s, T_f$  or  $T_d$  with probability 1 assuming there is no other transmission immediately following the current one. Thus, we have

$$\begin{cases} P_{ii} = 1 - (P_{is} + P_{if} + P_{id}) \\ P_{fi} = P_{si} = P_{di} = 1 \end{cases} \quad (10)$$

Furthermore, we denote  $p_w = P_{is} + P_{if}$ , which is the transmission probability of any node in the next time slot given that channel is sensed idle. The value of  $p_w$  can be obtained from the analysis of the collision avoidance algorithm in [9]. In our case, we assume for simplicity that the contention window size (CW) is held constant and hence  $p_w$  is fixed. From [9], this is given by

$$p_w = \frac{2}{CW + 1} \quad (11)$$

In the computation of transition probabilities for the above Markov model, the status of surrounding nodes needs to be considered since the channel is, in principle, shared with all neighbors of the reference node implicitly coupling their respective status. In [13], it is assumed that when the channel around A is sensed idle, the transmission probability in the next time slot of all neighbors of node A equals to that of node A (i.e.  $p_w$ ) which is reasonable if all the nodes within the carrier sensing range of node A are synchronized. However, with increasing distances between neighboring nodes, the difference between their channel status will become pronounced due to their large non-overlapping carrier sensing area; thus the transmission probability in the next time slot of these nodes may be lower than  $p_w$ , since they may be in the deferring state. Therefore, the transition probabilities of our Markov chain are computed based on the assumption when the channel around node A is sensed idle, the nodes within the transmission range of node A share the same channel status as node A; however the status of all neighboring nodes outside the transmission range of node A in the next time slot are statistically independent of the current channel status of node A. With this assumption, when the channel around node A is sensed idle, the transmission probability of the neighboring nodes within and outside the transmission range of node A in the next time slot can be calculated using  $p_w$  and  $p$  (the average transmission probability per generic slot) derived in the following, respectively. These assumptions are shown to have minimal effect on our modeling results as shown later in Section 4.

<sup>2</sup> Generic implies that the duration of each time slot varies and the durations  $T_s, T_f$  and  $T_d$  need not to be integral multiples of  $T_i$ .

### A. Average transmission probability per generic slot

Let the limiting probabilities of the Idle, Success, Fail and Deferring states be denoted by:  $\pi_i, \pi_s, \pi_f, \pi_d$  respectively. Then we denote the average transmission probability per generic slot for each node as  $p$ , which is sum of the limiting probabilities of the Success and Fail state. From Figure 2, this is given by

$$p = \pi_s + \pi_f = p_w \cdot \pi_i \quad (12)$$

Furthermore, from Figure 2 we have

$$\pi_i = P_{ii} \pi_i + (\pi_s + \pi_f + \pi_d) \quad (13)$$

Hence, using the normalization  $\pi_i + \pi_s + \pi_f + \pi_d = 1$ :

$$\pi_i = \frac{1}{2 - P_{ii}} \quad (14)$$

$P_{ii}$  is the transition probability from state Idle to itself which is identical to the event that none of nodes (including the reference) within carrier sensing range  $X$  transmits in the next time slot (denoted as  $P_x$ ); this is given by

$$P_{ii} = P_x (1 - p_w) \quad (15)$$

For a 2-D Poisson distribution of the number of nodes within a given area and assumptions in Section 3,

$$\begin{aligned} P_x &= \sum_{i=0}^{\infty} (1-p)^i \frac{(\pi(X^2 - R^2)\lambda)^i}{i!} e^{-\pi(X^2 - R^2)\lambda} \\ &\cdot \sum_{i=0}^{\infty} (1-p_w)^i \frac{(\pi R^2 \lambda)^i}{i!} e^{-\pi R^2 \lambda} \\ &= e^{-\pi(X^2 - R^2)\lambda p} \cdot e^{-\pi R^2 \lambda p_w} \end{aligned} \quad (16)$$

Substituting  $\pi_i$  in (12) with (14-16), we get the average transmission probability per generic slot  $p$  as

$$p = p_w \cdot \frac{1}{2 - e^{-\pi(X^2 - R^2)\lambda p} \cdot e^{-\pi R^2 \lambda p_w} (1 - p_w)} \quad (17)$$

Equation (17) can be solved numerically for  $p$  for any given node density, the carrier sensing range (or PCS threshold) and contention window size.

### B. Performance analysis

We next derive expressions for the number of transmissions per node per second, the successful rate of packet transmission per node and the saturation throughput per node or per unit area that requires all the transition probabilities of Figure 2.

The transition probability from Idle state to Deferring state  $P_{id}$  is the probability that some of nodes within carrier sensing range  $X$  transmits in the next time slot but node A itself does not transmit. Thus,  $P_{id}$  is given by

$$P_{id} = (1 - p_x)(1 - p_w) \quad (18)$$

Next, the transition probability from state Idle to Success,  $P_{is}$ , can be calculated via:

$$P_{is}(d) = P_1 P_2 P_3(d) P_4(d) \quad (19)$$

where  $d$  is transmitter-receiver separation distance between node A and B,

$P_1 = \text{Prob}\{\text{node A transmits in the next time slot}\}$ ,

$P_2 = \text{Prob}\{\text{the destination node B does not transmit in the next time slot}\}$ ,

$P_3(d) = \text{Prob}\{\text{No intrinsic collision}\}$ ,

$P_4(d) = \text{Prob}\{\text{No collision due to hidden terminal during the transmission of node A}\}$ .

Obviously,  $P_1 = p_w$ . By the assumptions in Section 3: when the channel around node A is sensed idle, the transmission probability of the neighboring nodes within and outside the transmission range of node A in the next time slot can be calculated with  $p_w$  and  $p$  respectively; therefore we have  $P_2 = 1 - p_w$ . In addition,  $P_3(d)$  – the probability that no other nodes within both the interference range of node B and the carrier sense range of node A transmits in the next slot is given by

$$\begin{aligned} P_3(d) &= \sum_{i=0}^{\infty} (1-p)^i \frac{(\pi^2 - A(d) - B(d))\lambda)^i}{i!} e^{-(\pi^2 - A(d) - B(d))\lambda} \\ &\cdot \sum_{i=0}^{\infty} (1-p_w)^i \frac{(B(d)\lambda)^i}{i!} e^{-B(d)\lambda} \\ &= e^{-(\pi^2 - A(d) - B(d))\lambda p} \cdot e^{-B(d)\lambda p_w} \\ &= e^{-\pi(S_0^r/d)^2 - A(d) - B(d)\lambda p - B(d)\lambda p_w} \end{aligned} \quad (20)$$

where  $\pi^2 - A(d)$  is the area of the intersection of the interference range of node B and the carrier sense range of node A.  $B(d)$  is the area representing the intersection of the interference range of node B and the transmission range of node A. Similar to the calculation of  $A(d)$ ,  $B(d)$  is given by

$$B(d) = \begin{cases} \pi d^2 & (0 \leq d \leq d_2) \\ \pi d^2 - \beta I^2 - dR|\sin(\alpha)| + \alpha R^2 & (d_2 \leq d \leq \min\{R, d_3\}) \\ \pi R^2 & (d_3 \leq d \leq R) \end{cases}$$

with

$$\begin{aligned} d_2 &= \frac{1}{1 + S_0^r} R, d_3 = \frac{1}{S_0^r - 1} R \\ \alpha &= \cos^{-1}\left(\frac{R^2 + d^2 - I^2}{2dR}\right), \beta = \pi - \cos^{-1}\left(\frac{d^2 + I^2 - R^2}{2dI}\right) \end{aligned} \quad (21)$$

The probability of no collision due to hidden terminals during a transmission of node A,  $P_4(d)$  can be calculated assuming that the duration of a data transmission (not counting ACK packet duration) is  $N$  times the average length of a generic slot time, i.e.

$$P_4(d) = \left( \sum_{i=0}^{\infty} (1-p)^i \frac{(A(d)\lambda)^i}{i!} e^{-A(d)\lambda} \right)^{2N} \quad (22)$$

$$= e^{-2A(d)\lambda p N}$$

Both  $P_3(d)$  and  $P_4(d)$  depend on transmitter-receiver separation distance  $d$  that is a random variable; therefore, we will average them based on the probability density function (PDF) of  $d$  for  $P_{is}$ . We assume that a node chooses any of its neighbors as its destination within its transmission range equiprobably and we do not consider the retransmission of collision packets.<sup>3</sup> Thus, according to the characteristic of two-dimensional Poisson distribution, we obtain the PDF of the distance between a node and its neighboring nodes within the Transmission Range  $R$  (one-hop distance), which is given by

$$f(d) = \frac{2d}{R^2} \quad (0 < d < R) \quad (23)$$

Hence

$$P_{is} = \int_0^R f(d) P_{is}(d) dd = \int_0^R f(d) P_1 P_2 P_3(d) P_4(d) dd$$

$$= p_w (1 - p_w)$$

$$\cdot \int_0^R \frac{2d}{R^2} e^{-(\pi(S_0 \frac{1}{\gamma} d)^2 - A(d) - B(d))\lambda p - B(d)\lambda p_w} e^{-2A(d)N\lambda p} dd \quad (24)$$

The probability of successful packet transmission per node can be found by

$$P_{success} = (1 - p_w)$$

$$\cdot \int_0^R \frac{2d}{R^2} e^{-(\pi(S_0 \frac{1}{\gamma} d)^2 - A(d) - B(d))\lambda p - B(d)\lambda p_w} e^{-2A(d)N\lambda p} dd \quad (25)$$

The transition probability  $P_{if}$  is equal to

$$P_{if} = p_w - P_{is} \quad (26)$$

Now, with the above transition probabilities of the Markov chain described earlier, we can get the limiting probability of the Idle, Success, Fail and Deferring state:  $\pi_i, \pi_s, \pi_f, \pi_d$  as follows:

$$\begin{cases} \pi_i = \frac{1}{1 + P_{if} + P_{is} + P_{id}}, \pi_f = \frac{P_{if}}{1 + P_{if} + P_{is} + P_{id}} \\ \pi_s = \frac{P_{is}}{1 + P_{if} + P_{is} + P_{id}}, \pi_d = \frac{P_{id}}{1 + P_{if} + P_{is} + P_{id}} \end{cases} \quad (27)$$

Finally, we can derive the other two performance indices: the number of transmission per node per second and the saturation throughput per node or per unit area. Recall that the duration of each Idle, Success, Fail and Deferring states

( $T_i, T_s, T_f, T_d$  respectively) can be calculated according to IEEE 802.11 specifications [16][17] as below:

$$\begin{cases} T_i = \delta \\ T_s = \frac{PHY_{hdr}}{v_h} + \frac{MAC_{hdr} + L}{v} + SIFS + \sigma + \frac{PHY_{hdr}}{v_h} + \frac{ACK}{v} + DIFS + \sigma \\ T_f = \frac{PHY_{hdr}}{v_h} + \frac{MAC_{hdr} + L}{v} + DIFS + \sigma \\ T_d = T_s \end{cases} \quad (28)$$

where  $\delta$  is the length of an empty slot time defined in the IEEE 802.11 standard,  $\sigma$  is propagation delay,  $L$  is the packets length in bytes,  $PHY_{hdr}$  is the header of physical layer and  $MAC_{hdr}$  is the header of MAC layer.  $\frac{PHY_{hdr}}{v_h}$  is the

transmission time of PLCP preamble and PLCP header, and its value can be found in TABLE I. For simplicity, we assume  $T_d = T_s$ , which means that the duration of each deferring interval is the same length as a successful transmission.

Then, it can be shown that the number of transmissions per node per second can be expressed as

$$N_t = \frac{\pi_s T_s}{\pi_i T_i + \pi_s T_s + \pi_f T_f + \pi_d T_d} \times \frac{1}{T_s} \quad (29)$$

$$+ \frac{\pi_f T_f}{\pi_i T_i + \pi_s T_s + \pi_f T_f + \pi_d T_d} \times \frac{1}{T_f}$$

which is the sum of the number of successful and unsuccessful transmission attempts for a node within unit time. Clearly with increasing  $N_t$ , more simultaneous transmissions are expected in the network.

TABLE I. PARAMETERS USED IN ANALYSIS AND SIMULATION

MAC Header	240bits
Transmission time of PHY Header	192μs(1Mb/s),96μs(2.5,5,11Mb/s)
ACK Length	112bits
Data Transmission Rate	1 Mb/s, 2 Mb/s, 5.5 Mb/s, 11Mb/s
Propagation Delay	1μs
SIFS	10μs
Slot Time	20μs
DIFS	50μs
SNR Threshold $S_0$	11dB(1Mp/s) or 21dB(11Mp/s)
Path loss exponent $\gamma$	3 or 2
Packets length $L$	1024 bytes or 300 bytes
Contention window size	1024 or 128
Transmission range $R$	25m or 35m
Node density $\lambda$	1/400 or 1/200 (per square meter)

The average saturation throughput per node (total successful transmissions from each node within unit time) can be evaluated by

$$TH_n = \frac{\pi_s L}{\pi_i T_i + \pi_s T_s + \pi_f T_f + \pi_d T_d} \quad (30)$$

and the aggregate saturation throughput per unit area

<sup>3</sup> Packet retransmissions lead to variations in the number of transmissions to different destinations due to different collision rate.

$$TH_u = TH_n \cdot \lambda = \frac{\pi_s L \lambda}{\pi_i T_i + \pi_s T_s + \pi_f T_f + \pi_d T_d} \quad (31)$$

Then, the aggregate saturation throughput of a region with area  $S$  is

$$TH = TH_u \cdot S = TH_n \cdot \lambda \cdot S \quad (32)$$

Further,  $N$  (the ratio between the duration of a data packet transmission and the average slot time) can be estimated by

$$N = \frac{T_{data}}{\pi_i T_i + \pi_s T_s + \pi_f T_f + \pi_d T_d} \quad (33)$$

where  $T_{data}$  is the duration of a data packet transmission, which equals  $\frac{PHY_{hdr}}{v_h} + \frac{MAC_{hdr} + L}{v}$ . The above requires the limiting

probability of each state; this can be obviated by the approximation below in (34) without incurring much accuracy loss since  $T_s, T_f$  and  $T_d$  are approximately the same. Hence, we have

$$N \approx \frac{T_{data}}{\frac{1-p_{ii}}{2-p_{ii}} T_d + \frac{1}{2-p_{ii}} T_i} \quad (34)$$

#### IV. ANALYTICAL AND SIMULATION RESULTS

We implemented numerical computations of Markov chain model with MATLAB [20] to examine how PCS threshold affects network performance under different settings for packet length, node density, data rate, contention window size, transmission range and path loss exponent. We also conducted extensive simulations via network simulator OPNET [19] to study the validity of the analytical model to validate the assumptions invoked in analysis.

##### A. Simulation set-up

We use an extended OPNET kernel module developed for [6, 7], which supports tunable PCS threshold, configurable propagation environment, and multiple 802.11b data rate in the simulation. The standard OPNET model for IEEE 802.11 calculates the SNR at each receive node by accumulating the interference from all concurrent transmissions. However, the sampling of PCS module only compares the strongest signal received with PCS threshold to decide whether to transmit. The modules of [6, 7] accumulate the signal power from all concurrent transmissions as the sampled power, which provide us a more accurate PCS model to study spatial reuse via simulation.

One particular concern in our simulation is the *boundary effect*, whereby the nodes on the boundary acquire more chance to transmit and experience less collision comparing with nodes in the network center. This causes estimates (e.g. aggregate throughput) to be positively biased. In order to reduce this boundary effect, we generate large scale networks

over a circular area<sup>4</sup>. Thus we use 2-D homogeneous Poisson distribution over a circular area of radius 150m as our network topology. The two-dimensional homogeneous Poisson distribution was simulated using the method presented in [15].

In the simulation, following our definitions in Section 3, we focus on the three main performance indices; namely

- Number of transmissions per node per second,  $N_t$
- Successful rate of packet transmission per node,  $p_{success}$
- Aggregate saturation throughput of the network,  $TH$

For each simulation scenario, saturated nodes send traffic with equal power to all its neighbors within their transmission ranges. Each data point on a simulation curve corresponds to 30 seconds of data traffic. All parameters used in both computation and simulation can be found in Table 1. Retransmission of lost packets is not allowed as already discussed in Section 3.

##### B. Simulation vs analytical results

Our first set of experiments was conducted for the data rate of 1Mbps, transmission range  $R = 25m$ , path loss exponent  $\gamma = 3$  and contention window size  $CW = 1024$ . In all the figures of this section, the X axis represents the normalized PCS threshold  $\beta$  defined as the ratio between the actual PCS threshold  $P_c$  and the reception sensitivity  $P_R$  in dB.

Figure 3 (a) shows that the number of transmissions per node per second when the node density  $\lambda$  is 1/400 per square meter and packet length  $L = 300$  bytes. We selected three representative values  $M, M+5, M-5$  ( $M=177$  for  $\lambda=1/400$ ), where  $M$  is the average number of nodes in the two-dimensional homogeneous Poisson distribution. In each case, we generate several topologies for simulation; we only show the result from one topology as it was found to be typical.

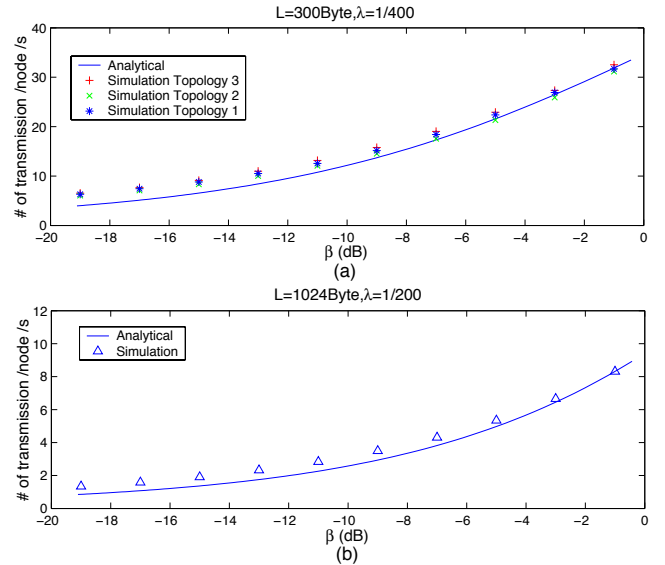


Figure 3. Number of transmissions per node per second as a function of PCS threshold for Data Rate = 1Mbps

<sup>4</sup> When the node density  $\lambda$  is 1/400 per square meter, the average number of nodes within the circular area is 177.

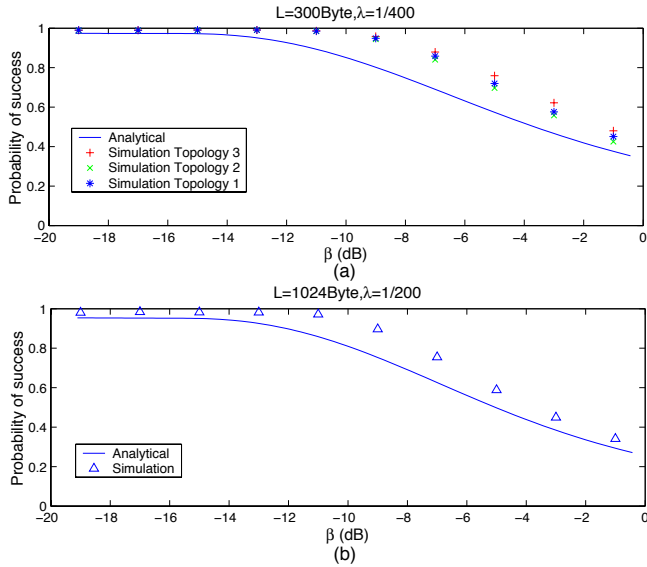


Figure 4. Successful rate of packet transmission per node as a function of PCS threshold for Data Rate = 1Mbps

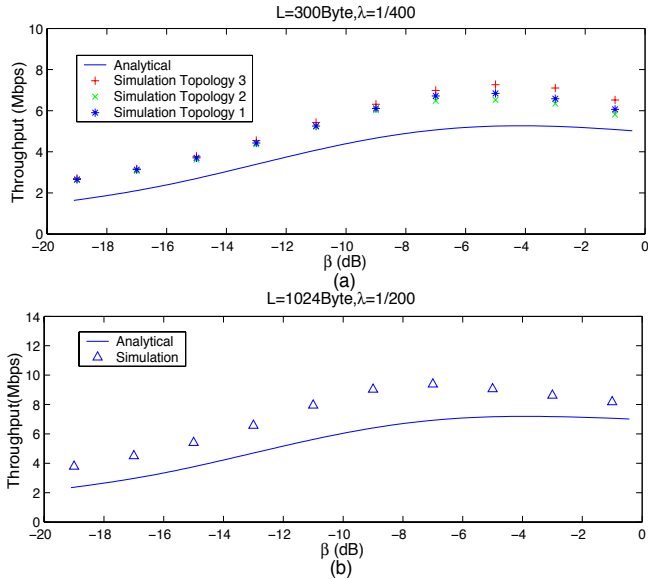


Figure 5. Saturation throughput of the whole network as a function of PCS threshold for Data Rate = 1Mbps

From Figure 3(a), as  $\beta$  increases (i.e. PCS threshold increases and carrier sensing range decreases), the number of transmissions per node per second (and number of simultaneous transmissions) increases greatly. The reason is that with shorter carrier sensing range, the nodes freeze their backoff counters less frequently. Figure 3(b) show the number of transmissions per node per second when the node density  $\lambda$  doubles and packet length  $L$  is increased to 1024 bytes.

Figure 4 shows the successful rate of packet transmission per node for the same two cases as Figure 3. As the PCS threshold increases, the successful rate of packet transmissions per node drops significantly. The reason is that with shorter

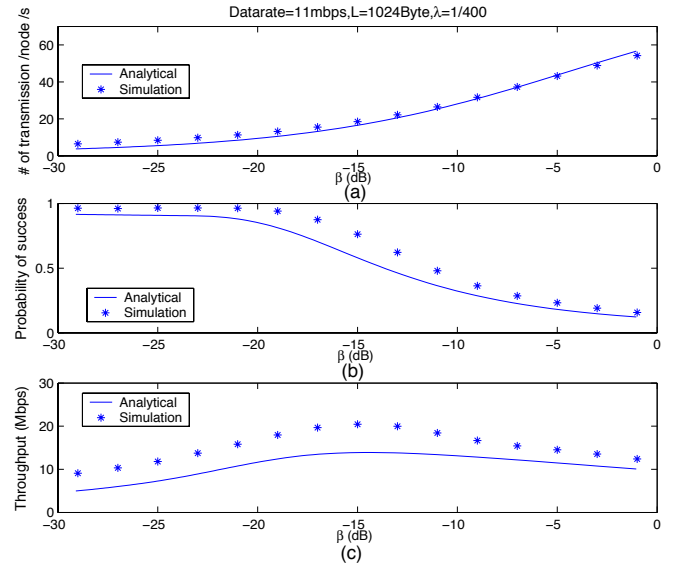


Figure 6. Performance indices as a function of PCS threshold for Data Rate = 11Mbps

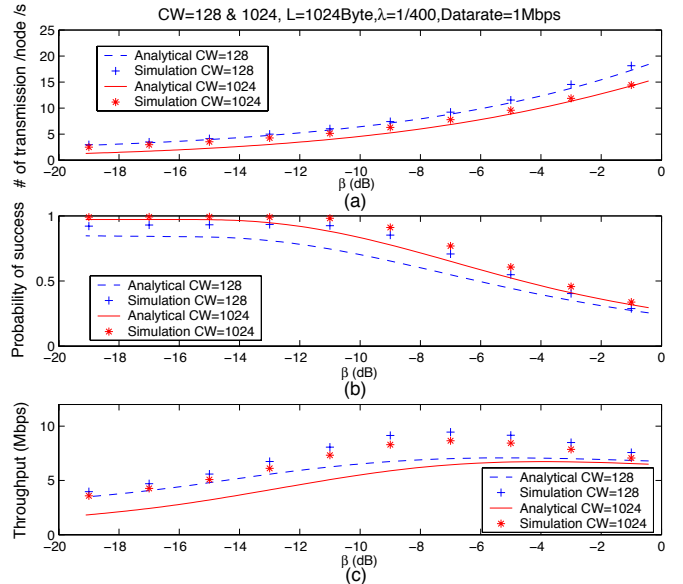


Figure 7. Performance indices as a function of PCS threshold for different contention window

carrier sensing range, the hidden area increases and hidden terminals problem occurs more frequently. In both cases, the analytical curve matches the tendency of simulation results well.

Figure 5 shows the aggregate saturation throughput of the network for the same two cases as Figure 3. Where  $TH_u$  is maximum indicates an optimal value of  $\beta$  that balances the trade-off between the amount of spatial reuse and the probability of packet collisions. Also, the differences between the analytical results and the simulations are worth remarking. We find that the main reason for this gap is the network boundary effect in simulations. The effect is more significant when PCS threshold is lower, because in these cases the

boundary nodes grab much more opportunities of transmissions which do not belong to the circular area if there are nodes outside. We observe that as we decrease the scale of network, path loss exponent or increase transmission range, the border effect becomes more pronounced. But in all cases, the analytical curves capture the broad trends of simulation results, which verifies the effectiveness of the analytical model. The approximating assumptions in our analysis are the second source of the difference. In the definition of  $I$  and  $X$ , only the signal power from a single node is considered, which is not true in our simulation for high density networks.

Our second set of experiments was conducted for the highest data rate of 802.11b – 11Mbps. We use the same parameters as those of the first group, except that  $\lambda$  is 1/400 per square meter;  $L=1024$  bytes and data rate is 11Mbps. Figure 6 shows the performance indices as a function of PCS threshold. Due to the increase of SNR required by higher data rate, the  $\beta$  for optimal throughput has changed to -15dB. But as we can see, the analysis model can still predict the trends in simulation results.

Finally, we show an experiment with different contention window size. We use the same parameters as those of the first set, except that  $\lambda$  is 1/400 per square meter;  $L=1024$  bytes; and  $CW=1024$  or 128. Figure 7 shows the performance indices as a function of PCS threshold. In the figures 7(b), when  $\beta$  is lower than -13dB, the collisions due to hidden terminals is almost zero but there are still significant packet loss in both simulation and analytical curves for  $CW=128$ . The loss results from the fact that some nearby nodes select the same slot to transmit. Therefore, besides the collisions that are due to hidden terminals, the analysis can also incorporate intrinsic collisions as well.

## V. CONCLUSION

In this paper we presented a novel approach in evaluating the effect of PCS threshold on the performance of ad hoc networks. The contribution of this work is the development of an analytical model that describes how PCS threshold affects the saturation throughput and the probability of packet collisions with randomly distributed nodes. In addition, we have shown that our analytical results, under different scenarios with different parameters, capture the tendency of the simulation curves well, which prove the effectiveness of this model.

## REFERENCES

- [1] X. Guo, S. Roy, W. Steven Conner, "Spatial Reuse in Wireless Ad-Hoc Networks," VTC2003.
- [2] F. A. Tobagi and L. Kleinrock, "Packet Switching in Radio Channels: Part II - The Hidden Terminal Problem in Carrier Sense Multiple Access and the Busy Tone Solution," vol. COM-23, no. 12, pp. 1417-1433, 1975.
- [3] D. Shukla, L. C. Wadia, S. Iyer, "Mitigating the exposed node problem in IEEE 802.11 adhoc networks," IEEE ICCCN, October 2003

- [4] K. Xu, M. Gerla, S. Bae, "How effective is the IEEE 802.11 RTS/CTS handshake in ad hoc networks?" GLOBECOM '02, Nov. 2002
- [5] F. Ye, S. Yi and B. Sikdar, "Improving Spatial Reuse of IEEE 802.11 Based Ad Hoc Networks," GLOBECOM '03. December 2003.
- [6] J. Zhu, X. Guo, L. L. Yang, and W. S. Conner, "Leveraging Spatial Reuse in 802.11 Mesh Networks with Enhanced Physical Carrier Sensing," ICC '04, June 2004.
- [7] J. Zhu, X. Guo, L. Lily Yang, W. Steven Conner, S. Roy, Mousumi M. Hazra, "Adapting physical carrier sensing to maximize spatial reuse in 802.11 mesh networks," Wireless Communications and Mobile Computing Volume 4, Issue 8, p 933-946, December 2004
- [8] X. Yang and N. H. Vaidya, "On Physical Carrier Sensing in Wireless Ad Hoc Networks", INFOCOM 2005, March 2005.
- [9] G. Bianchi, "Performance analysis of the IEEE 802.11 distributed coordination function," IEEE Journal on Selected Areas in Communications, Vol. 18, No. 3, pp. 535 -547, March 2000
- [10] F. Cali, M.Conti, and E.Gregori, "Dynamic tuning of the IEEE 802.11 protocol to achieve a theoretical throughput limit," IEEE/ACM Transactions on Networking, Vol. 8, No. 6, Dec. 2000
- [11] H. Takagi and L. Kleinrock, "Optimal transmission range for randomly distributed Packet radio terminals," IEEE Trans. on Commun. vol. Com-32, No. 3, Mar., 1984, pp 246-257
- [12] L. Wu and P. K. Varshney, "Performance analysis of CSMA and BTMA protocols in multihop networks (i). single channel case," Information Sciences, vol. 120, pp. 159-177, November 1999.
- [13] S. Gabriel, R. Melhem, and D. Mosse., "A unified interference/collision analysis for power-aware adhoc networks," INFOCOM 2004, March 2004.
- [14] J. Deng , B. Liang, and P. K. Varshney, "Tuning the Carrier Sensing Range of IEEE 802.11 MAC," Globecom'04, November 29 - December 3, 2004
- [15] D. Stoyan and W.S. Kendall, "Stochastic geometry and its applications," Chapter 2, Chichester ; New York : J. Wiley, c1995
- [16] IEEE P802.11. Standard for Wireless LAN Medium Access Control (MAC) and Physical Layer (PHY) Specifications, 1997.
- [17] IEEE P802.11b. Supplement to Standard IEEE 802.11, Higher speed Physical Layer (PHY) extension in the 2.4GHz band, 1999.
- [18] IEEE P802.11a. Supplement to Standard IEEE 802.11, High speed Physical Layer (PHY) extension in the 5GHz band, 1999.
- [19] <http://www.opnet.com>
- [20] <http://www.mathworks.com/>